



Concentric tubular steel braces subjected to seismic loading: Finite element modeling



Madhar Haddad

Department of Architectural Engineering, United Arab Emirates University, P. O. Box 15551, Al Ain, United Arab Emirates

ARTICLE INFO

Article history:

Received 22 February 2014

Accepted 10 October 2014

Available online 29 October 2014

Keywords:

Finite element model

Concentric tubular steel braces

Cyclic behavior

Ultra-low-cycle fatigue

Cumulative plastic strain

Fracture

ABSTRACT

Steel buildings are susceptible to damage during earthquakes if an unreliable bracing system is used. A well-designed and detailed concentric bracing system is needed for steel buildings in a seismically active area. Failure of a concentric bracing member occurs at the mid-length plastic hinge. A refined finite element model has been developed to simulate the hysteresis behavior of bracing members under cyclic loading including fracture. The model provides similar hysteresis behavior to previous (Shaback and Brown [1]) and two new experiments (Tremblay et al. [2]). The specimens were subjected to different loading protocols. It was found that an initial imperfection affects the pre-buckling and first buckling cycles but has no effect on the following cycles. The greater the initial yield stress of the HSS, the earlier is the occurrence of local buckling. The cumulative plastic strain is greater at the outer surface than at the inner surface of the compressive corners/web of the mid-length plastic hinge where fracture initiates. Significant local rotation follows the same trend as the significant plastic strain of the same element where fracture initiates.

© 2014 Elsevier Ltd. All rights reserved.

1. Introduction

Concentric braces can be used in steel and concrete buildings to minimize lateral storey drift by absorbing the input energy of wind and ground movements. Under these movements, lateral drift is greater in unbraced buildings than in braced buildings. For symmetrical inelastic lateral loading history, lateral drift for a single diagonal brace is less in tension than in compression due to brace buckling (the behavior of concentric braces is different in tension from compression). Therefore, concentric braces are commonly used in opposing pairs in buildings in one bay or in adjacent bays.

Hollow structural steel sections (HSS) have been frequently tested under reversed axial displacements, as such sections are popularly used as bracing elements. The objective is to understand the hysteresis behavior and predict the fracture life of such members in an attempt to improve the performance of these braces when buildings are exposed to seismic excitations. These tests (Jain et al. [3]; Black et al. [4]; Lee and Goel [5]; Liu and Goel [6]; Tang and Goel [7]; Walpole [8]; Shaback and Brown [1]; Tremblay et al. [9]; Elchalakani et al. [10]; Goggins et al. [11]; Uriz [12]; Yang and Mahin [13]; Fell et al. [14,15]; Han et al. [16]; Tremblay et al. [2]; Haddad et al. [17]; Roeder et al. [18]; Takeuchi and Matsui [19]; lai and Mahin [20]) have revealed that fracture occurs after a few (1 to 4) cycles of local buckling due to the high strains and rotations at the compressive corners/web of the mid-length plastic hinge. After the brace has buckled, most of the tensile elongation and inelastic strains occur within the mid-length plastic hinge region.

Finite element models have been developed for the same purposes. The model of Haddad et al. [21] suggested that fracture life is related to the total axial displacements without repeating the unloading parts of cycles. The crack void growth model (CVGM) with the triaxiality effect of strains is also able to predict the fracture life of HSS bracing members (Kanvinde and Deierlein [22]; Myers et al. [23]; Fell et al. [15,24]). A modified CVGM model is tested here for the CAN/CSA-40.21-98, class C, Grade 350 W [25] and for ASTM A500, Grade C [26], steel tubular braces (HSS) under cyclic loadings. Another objective of the current work is to provide a refined material model that is able to predict the exact hysteresis behavior and to overcome a shortcoming of previous models, specifically the overshoots in the axial compressive resistance. The effect of an initial imperfection on the hysteresis behavior of HSS braces is investigated.

2. Design of specimens

All specimens (1B, 2A, 2B, 3A, 3B, 3C, 4A, 4B) of the Shaback and Brown tests [1] listed in Table 1 were designed according to the CAN/CSA-S16.1-94 (CSA 1994) standard [27] except for the fillet weld, which was designed according to Korol [28]. The tensile capacity of the connection (gusset plate) is greater than the tensile capacity of the specimen. Rectangular gusset plates were inserted into longitudinal slots in the flanges of the HSS at both ends. The gusset plates were welded to the HSS along the slot. The front end of the gusset plate was welded to the HSS at the slot. Hence, no cover plates were used at the net section of the brace.

E-mail address: madhar@uaeu.ac.ae.

Table 1
Properties of the HSS specimens, gusset plates and fillet weld.

Specimen	HSS section, (mm)	HSS length (mm)	Total specimen length, L , (mm)	Gusset plate cross sectional area, $w_g t_g$, (mm ²)	Fillet weld length, L_w , (mm)	HSS E (GPa)	HSS F_y (MPa)
1B ¹	127 × 127 × 8	3350	3452	5715	300	191	421
2A	152 × 152 × 8	3950	4040	6350	350	202	442
2B	152 × 152 × 9.5	3950	4028	7620	350	196	442
3A	127 × 127 × 6.4	4350	4456	5080	300	196	461
3B	127 × 127 × 8	4350	4446	5715	300	191	421
3C	127 × 127 × 9.5	4350	4414	6350	300	202	461
4A	152 × 152 × 8	4850	4944	6350	350	202	442
4B	152 × 152 × 9.5	4850	4914	7620	300	196	442
RHS-19 ²	152 × 152 × 9.5	3829	3905	11,201	290	200	345 ^a
CHS-1	273 × 9.5	4109	4198	13,068	450	235	317 ^a

CAN/CSA-40.21-98, Class C, Grade 350 W. Rectangular gusset plates, F_y (gusset plate) = 300 MPa (hot rolled). Asymmetrical displacement history. E480XX Electrode. ASTM A500, Grade C. Tapered gusset plate, ASTM A572 Grade 345. Symmetrical displacement history. E490 XX Electrode. ^a Specified minimum yield stress.

¹ Shaback and Brown [1].

² Tremblay et al. [2].

Similarly, a slotted connection was adopted for specimens RHS-19 and CHS-1 of the tests by Tremblay et al. [2], listed in Table 1. For these connections, the net section at the end of the slots was reinforced with cover plates to avoid fracture at this critical location. The connections were designed and sized according to the AISC 2005b [29] and the AISC seismic provisions [30], respectively. The gusset plate dimensions a and b are obtained following the modified Uniform Force Method using the minimum possible gusset plate thickness t_g with the working point being located at the intersection of the beam bottom flange and the adjacent column inner flange to minimize the gusset plate dimensions (Sabelli [31]). All failure modes are verified including net section fracture including shear lag effects, tear-out failure in the brace and in the gusset plate, tension yielding on the Whitmore section of the gusset plate, and failure of the welds.

The optimal brace inclination angle for maximum shear rigidity with respect to the horizontal axis of Tremblay [2] tests is $\theta = 35^\circ$ (Moon et al. [32]). The results of design for all specimens are listed in Table 1 and in the figures in the Appendix. For RHS-19 and CHS-1, $a = 513$ mm and $b = 359$ mm.

3. Loading protocols

All specimens analyzed herein were subject to quasi-static cycles of reversed axial displacements. Two displacement protocols were used: the first is asymmetric in the experiments of Shaback and Brown [1] and the second is symmetric in the experiments of Tremblay et al. [2] as shown in Fig. 1(a) and (b). For the Tremblay et al. specimens, the loading sequence was developed in terms of interstorey drift. The maximum normalized axial deformation of all braces is shown in Fig. 1(c). The axial deformation of the brace is normalized with respect to the brace length between the end hinges, L_H .

4. Finite element model description

The use of a four-node quadrilateral shell element (S4R) in modeling steel braces accounts for large strains and rotations and allows for changes in thickness with deformation. S4R is a reduced integration element with three translational and three rotational degrees of freedom per node. This element is suitable for analyzing thin and thick members. Seven integration points were adopted through the thickness of the S4R element so that the nonlinear stress distribution was estimated. Triangular shell elements were avoided since they can behave in too stiff a manner. A high mesh density with element size less than the thickness of the HSS was used at the mid-length plastic hinge. The element aspect ratio in this region was 1. The number of (nodes, elements) used in modeling each specimen of the Shaback and Brown tests [1], RHS-19

and CHS-1 are (16730, 13580), (23218, 20246), and (17818, 15362), respectively.

The gusset plates were connected to the HSS by the nodes on their interfaces. The cover plates, if present, were connected to the HSS by tie-type multi-point constraints (MPC) at nodes on the longitudinal sides of each cover plate. Fixed brace end conditions were used at both ends of the specimens. Neither the weld nor the slotted hole was modeled. The

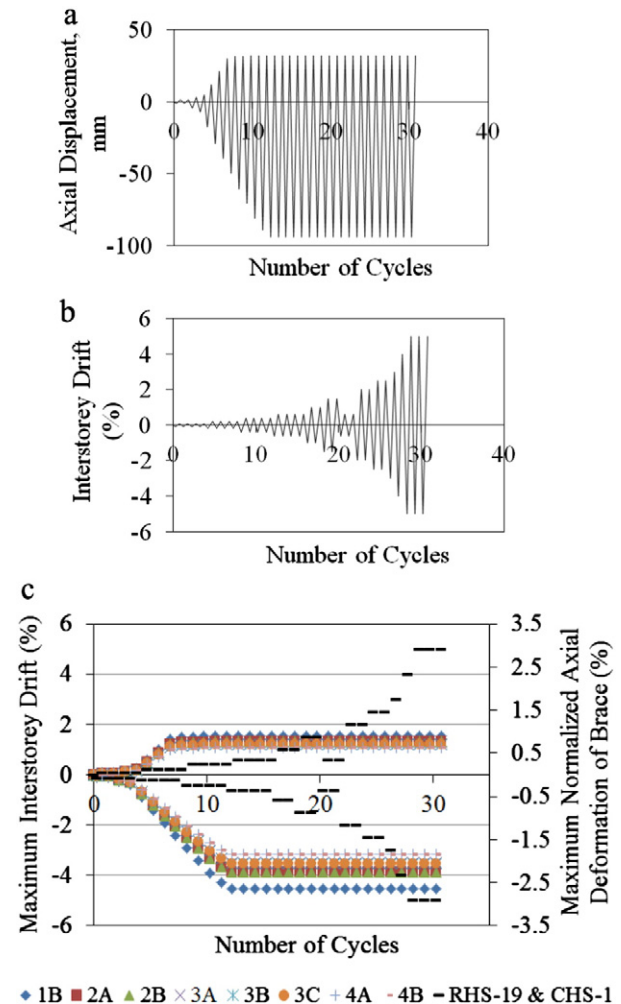


Fig. 1. Displacement protocols for specimen 4A (a), RHS-19 and CHS-1 (b), and maximum amplitudes for tests of Shaback and Brown [1] and Tremblay et al. [2], (c).

Download English Version:

<https://daneshyari.com/en/article/284585>

Download Persian Version:

<https://daneshyari.com/article/284585>

[Daneshyari.com](https://daneshyari.com)